
IMPROVED K -MER BASED PREDICTION OF PROTEIN-PROTEIN INTERACTIONS WITH CHAOS GAME REPRESENTATION, DEEP LEARNING AND REDUCED REPRESENTATION BIAS

A PREPRINT

Ruth Veevers 

The Sainsbury Laboratory
Norwich, NR4 7UH

Dan MacLean 

The Sainsbury Laboratory
Norwich, NR4 7UH
dan.maclean@tsl.ac.uk

October 24, 2023

ABSTRACT

Protein-protein interactions drive many biological processes, including the detection of phytopathogens by plants' R-Proteins and cell surface receptors. Many machine learning studies have attempted to predict protein-protein interactions but performance is highly dependent on training data; models have been shown to accurately predict interactions when the proteins involved are included in the training data, but achieve consistently poorer results when applied to previously unseen proteins. In addition, models that are trained using proteins that take part in multiple interactions can suffer from representation bias, where predictions are driven not by learned biological features but by learning of the structure of the interaction dataset.

We present a method for extracting unique pairs from an interaction dataset, generating non-redundant paired data for unbiased machine learning. After applying the method to datasets containing *Arabidopsis thaliana* and pathogen effector interactions, we developed a convolutional neural network model capable of learning and predicting interactions from Chaos Game Representations of proteins' coding genes.

1 Introduction

Phytopathogens are a major threat to global crop production. The fungal phytopathogen *Magnaporthe oryzae* that causes cereal blast is responsible for around 30% of rice production loss and has now emerged as a pandemic problem on wheat (Nalley et al. 2016). The oomycete *Phytophthora infestans* causes losses of around 6 billion USD to potato production, annually (Haas et al. 2009). The bacterium *Ralstonia solanacearum* has a wide host range and can cause losses of over 30% in potato, banana and groundnut (Yuliar, Nion, and Toyota 2015). The incidences of crop disease are increasing as global climate change and agricultural practice are expanding the geographical range of pathogens and upping the stakes in the evolutionary arms race.

Plant detection of pathogen infection occurs at two levels: the cell surface where pathogen molecules (PAMPs) are detected by a family of Receptor Like Kinase (RLK) cell surface receptors to trigger immune response and also intracellularly where pathogen effectors can interact with R-Proteins that trigger the immune response. Identifying interacting RLK/PAMPs and Effector/R-Proteins is a key part of immunity research. On the plant side, RLKs and

R proteins are well characterised and can be identified bioinformatically. On the pathogen side PAMPs and effector proteins are the shock troops of infection, manipulating the host at the infection interface to the pathogens advantage. Identifying and characterising a pathogen's effector content is a critical first step in understanding diseases and developing resistance, but until recently effectors were notoriously difficult to characterise from sequence data. In most phyla they have only a few easily determined sequence characteristics (some in fungi are cysteine rich or have a MAX motif, some in oomycetes have the RXLR motif or WY fold) but in many cases no sequence identifiers are known (Franceschetti et al. 2017).

To understand infection processes, to provide genome-level understanding of the functions of this important class of genes and to develop future disease resisting crop varieties and agricultural management strategies there is a critical need to identify PAMP-RLK and effector-R gene complements and immune triggering pairings computationally from genome and protein sequence data.

Kristianingsih and MacLean (2021) recently developed class-leading deep learning based models for effectors that perform classification of effectors across species and phyla with an accuracy greater than 90%. This removed the need for older computational pipelines with in-built *a priori* assumptions about what might constitute an effector sequence in the absence of sequence features known to group them (Sperschneider et al. 2015). A significant aspect of these models is that training set sizes were on the order of 100-200 input sequences, demonstrating that with appropriately parameterized and optimized architectures, deep learning can be successfully applied despite apparently low sample sizes.

1.1 Prediction of PPIs

The utility of PPIs such as these has led to the development of several tools for the prediction of new ones in order to discover proteins that may interact with a given target protein. Molecular dynamics simulations can model the physics underlying proteins' behaviours to simulate how they may interact. However, these simulations come at a high computational cost, particularly when attempting to model an event as specific and potentially rare as these interactions, making the method unsuitable for large-scale searches.

There is considerably more primary sequence data than structural data known regarding proteins, and so methods for prediction of interactions that require only sequence data have been developed. Following the success of AlphaFold2(Jumper et al. 2021) in predicting protein structure from sequence, there have been attempts to apply the AlphaFold model to other problems. AlphaFold-Multimer(Evans et al. 2021) predicts complexes formed by multiple protein chains, and AlphaPulldown(Yu et al. 2022) builds this into means of searching for interactions in large databases.

Sequence data has been encoded for machine learning as k -mer counts or as one-hot encoding. Convolutional Neural Networks (CNNs) have previously been applied to the problem. Sequence data has been augmented using using PSI-BLAST to derive input matrices for each protein containing probabilistic protein profiles or Position-Specific Scoring Matrices(Hashemifar et al. 2018) (Wang et al. 2019). Approaches including Hashemifar et al. (2018) use shared parameters in twinned(Bromley et al. 1993) architectures, training a single model to extract features from both components of the PPI. Ding and Kihara (2019) also incorporates physiochemical properties like side-chain charge and hydrophobicity.

Some methods of predicting from protein sequence have approached sequences using methods designed for handling language: creating doc2vec(Le and Mikolov 2014) encodings of a set of sequences to use as features(X. Yang et al. 2020), or building a protein language model through the use of transformers(Rao et al. 2021) (Rives et al. 2021). Qiu et al. (2020) incorporates both homology and language vector encoding for per-residue binding prediction.

S. Yang et al. (2019) apply existing PPI prediction methods to interactions between *Arabidopsis thaliana* and pathogen proteins and find that the methods do not translate well. They supplement their random forest model by explicitly including information about the network of interactions.

1.2 Representation bias

The paired input of PPI data introduces a potential source of bias. Each input sample consists of two proteins, so proteins could appear in multiple pairs. Park and Marcotte (2012) enumerate the ways that proteins can be combined into pairs: both proteins in a test pair might be part of the training set (in-network), or one might be previously unseen by the model, or they could both be unseen (out-of-network). Test sets that consisted of in-network proteins yielded better performance than those featuring out of network proteins. Hamp and Rost (2015) identify similar groups and concluded that the choice of test group dramatically affected the prediction results, while also identifying that including a given protein in multiple pairs in the training data lowers the accuracy on unseen test proteins compared to including it in a single training pair. Eid et al. (2021) examine the extent to which this has effected published machine learning studies, and demonstrate that models can achieve 0.99 AUC scores on existing benchmark datasets even when the

protein sequences have been masked such that biological features cannot contribute to prediction. They propose a comprehensive framework for identifying bias in PPI datasets.

As well as representation bias driven learning, the application of machine learning to biological sequences also requires consideration of the issue of data leakage from homology(Jones 2019). Pairs of sequences may correspond to related structures with very similar forms and functions despite differences in sequence(Rost 1999). The inclusion of homologous biomolecules appearing in both the testing and training data can result in overestimation of a model’s accuracy and poor generalization to other data. While sequence identity cannot fully identify all homologous proteins, a common approach used by recent studies in the prediction of PPIs(X. Yang et al. 2020), binding residues(Qiu et al. 2020), tertiary structures(Singh et al. 2019), and other biomolecular properties is to filter by sequence identity using software like CD-Hit(Li and Godzik 2006).

However, machine learning models are widely understood to require abundant training data. The naive method of sequence filtering for PPI prediction - clustering to a given sequence identity threshold and then discarding interactions until there are no pairs of interactions that use a protein from the same cluster - potentially discards more information than necessary to a degree that depends on the random seed.

1.3 Chaos Game Representation

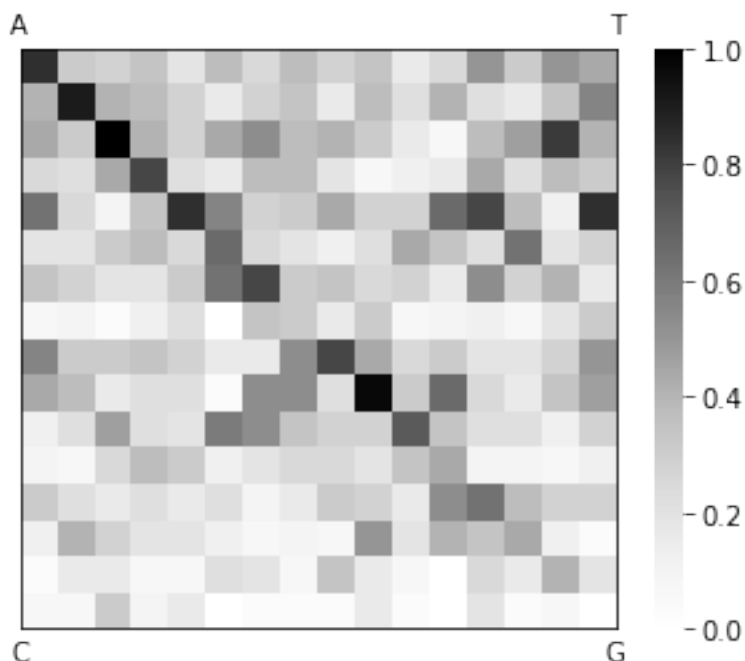


Figure 1: An example CGR attractor, built from the sequence of the Arabidopsis *CULA* gene (TAIR ID: AT5G46210.1) at a 4-mer resolution. This CGR incorporates frequency; the darkness of each pixel corresponds to a given 4-mer’s frequency in the sequence; each cell contains the number of times the 4-mer appears, normalised within each CGR image.

The Chaos Game Representation (CGR)(Jeffrey 1990) of a nucleotide sequence is a representation of the composition of a sequence as a 2-dimensional image. The “Chaos Game” is a process in which a sequence drawn from an alphabet of n characters can be represented as points in an n -sided polygon. Certain values of n produce fractal patterns given enough points, but when $n = 4$, the square produced is filled uniformly. To encode a genetic sequence, the four points of a CGR represent the four nucleotides and a point is added for each residue in the sequence. If the square is divided into quadrants, the number of points in each quadrant will be the number of times the nucleotide representing the nearest corner occurs in the sequence. Further division of the quadrants creates sub-quadrants, containing points corresponding to the occurrences of two-character-long subsequences (or 2-mers). This division and subdivision can be repeated to any value of k . By setting a value for k , CGRs can be represented as a 2-dimensional data structure in which each cell contains either booleans (to show presence or absence of a corresponding k -mer) or numbers (to show the number of times the k -mer occurs).

An example with frequency information included at 4-mer resolution is shown in Figure 1, which shows some visually identifiable indications of the composition of the sequence. The dark line along the diagonal shows an abundance of 4-mers that consist solely of “A” and “G” residues, whereas the lighter region along the bottom edge indicates that 4-mers of “C”s and “G”s in combination are more scarce.

A variety of methods have been proposed to encode sequences of amino acids as CGRs; Dick and Green (2020) implements four of these approaches for a taxonomic classification task: reverse mapping to standardised nucleotide sequences(Deschavanne and Tuffery 2008); two versions of representation via a 20-sided polygon with a point for each potential amino acid, with appearance of 9-mers represented either as a greyscale intensity or black-and-white binary; and a 20-flake frequency matrix chaos game representation(Löchel et al. 2020). The models performed similarly modestly. Jia et al. (2019) uses chaos game representation to build inputs for a PPI classifier, converting their protein sequences into pseudo-nucleic sequences by replacing each amino acid with a single representative codon following Deschavanne and Tuffery (2008) and counting frequencies of points within the regions of the CGR attractors to pass as input into an ensemble of random forest classifiers.

The 2-dimensional arrangement of k -mers representing a sequence is reminiscent of single channel images, and we have extended CGRs such that each array element contains an ordered 2-tuple of k -mer counts from 2 distinct sequences, analogous to a two-channel image. There has been extensive research into machine learning for the purposes of computer vision, resulting in powerful models capable of image processing tasks such as semantic segmentation and object recognition. When rendered as an image, a CGR displays recognisable visual patterns, suggesting that it would be amenable to use in deep-learning models effective in recognising patterns in images such as those based on Convolutional Neural networks (CNNs). In this work, we develop and train CNN architectures for the prediction of *Arabidopsis thaliana* PPIs from two-channel CGR tensors that represent the pair of gene sequences that code for the proteins. We extend this further using transfer learning, focusing specifically on interactions between *Arabidopsis thaliana* proteins and effectors. We also explore the ability of our models to identify features specific to taxonomic ranks, testing their performance by examining two metagenomics questions:

1.4 Augmentations and Synthetic data

While the image-like format of the CGR attractors proved well-suited to CNN models, the field of image processing using neural networks has developed methods beyond architectural considerations to improve models’ performance on tasks. On-the-fly augmentations, from simple transformations such as rotation and scaling to more complex blending of images(Xu et al. 2023), have assisted in the training of object detection and semantic segmentation neural networks. By showing the adjusting the training data during supervised learning, the model is exposed to more variety in its training data with the intent that it is more readily able to generalise to unseen test data.

Additionally, various studies have demonstrated methods of generating synthetic images. Supervised machine learning for image processing tasks like object detection require ground truth data from which to learn, but the per-pixel labelling of the contents of an image can be an expensive or time-consuming bottleneck, particularly if the labelling task calls for expert knowledge. Synthetic images present an opportunity to quickly produce both an image and its ground truth labels and gives researchers control over the contents of their training data which has been used to augment real training data in some domains(Man and Chahl 2022).

Cut-and-paste methods(Dwivedi, Misra, and Hebert 2017) take small numbers of manually labelled image components and position them on a background to vary the composition of a collection of images. While computationally simple, this has recently been successfully applied to plant phenotyping (Albert et al. 2021). Even more control over an image’s contents can be gained when the image is rendered using 3-dimensional modelling, though the process of creating and rendering the objects can still require significant time and expense. Researchers have used video game engines Unreal Engine(Epic Games 2023) and Grand Theft Auto V(Rockstar Games 2013) as well as bespoke engines to render environments(Saleh et al. 2018). Ward and Moghadam (2020) create 3D plants to render as top-down images along with segmentation masks for each leaf. Generative Adversarial Nets (GANs)(Goodfellow et al. 2014) create images using a pair of specialised and opposed neural networks, where one attempts to generate images that can pass as real and another attempts to identify whether an image is real. Each model improves as it trains which makes the other model’s task harder, driving improvement further. Shin et al. (2018) leverage this process not just to generate more training data but to anonymise medical photographs. The GAN model can be extended to Conditional Generative Adversarial Nets (cGANs)(Mirza and Osindero 2014) to generate images belonging to different classes, such as photographs of diseased and non-diseased plants(Abbas et al. 2021).

Training data for PPI models must be experimentally determined, which requires time, expense and expert knowledge. As such, exploiting existing data to further training poses a potential advantage. However, despite their image-like properties, standard methods of image augmentation such as rotation, cropping and scaling would not work for CGR

representations as they would change the underlying sequences such that the labels could no longer reliably be used as ground truth. We explore two methods of augmenting or generating synthetic CGR data.

2 Results

2.1 Graph-Reduction Algorithm for Non-redundant Datasets (GRAND) consistently retains more data than random discarding of duplicated samples

The issue of redundancy in biological sequence data caused by high sequence similarity is exacerbated in the case of PPI predictions, where each sample is composed of two sequences. The representation bias-driven learning that this can introduce may result in models that appear to perform well but which cannot generalise to new data. We enforce strict non-redundancy in the training and test datasets to remove this potential source of bias, to seek a model that can predict interactions from unseen, out-of-network sequences. However, a secondary priority is that since labelled, experimentally-derived interaction data is not trivial to obtain, we wish to retain as many samples as possible.

Figure 2 (a) shows the PPIs from ArabidopsisPPI represented as a network. Each node represents a cluster of one or more similar genes, from the output of CD-Hit. Each edge represents a known interaction between at least one pair of the proteins coded for by the genes contained within each cluster. A node’s degree is defined as the number of other nodes to which it is connected by an edge. Many of the genes’ products are included in multiple interactions; some nodes in the network have a degree of over one hundred. GRAND iteratively prunes this network until each remaining node has one single neighbour.

While any node has a degree greater than one, the following is repeated. Each node with degree one is taken in turn, and its sole neighbour is found. If the neighbour has other edges, they are removed. When no nodes with degree one remain, for each edge an “edge-sum” is calculated by summing together the degrees of the two nodes that it connects. The edge with the lowest edge-sum is selected for inclusion, and all other edges between the connected nodes and their other neighbours are dropped. Any nodes that are no longer connected by any edges are removed, and considered for inclusion as part of a negative pair. The dataset is then constructed from this network by choosing randomly one of the known interactions that each edge represents.

Figure 2 (b) shows the new network, wherein each node shares an edge with exactly one other node. This new network contains 1,106, whereas the network created by random discarding contained 867. This is a 27.6% increase in available non-redundant data.

The improvement holds for the other datasets to which we have applied GRAND. On the EffectorK host/pathogen effector interaction dataset, which contains 1,220 interactions between 769 CD-Hit clusters, 1,000 applications of the naive approach returns a mean of 131.62 interactions (standard deviation 5.26), where none of the attempts return more than 148 interactions. GRAND returns 183 interacting pairs, for a 23.6% increase over the maximum naive result and 39.0% increase over the mean. The larger HPIDB dataset contains 36,139 interactions between 13,099 CD-Hit clusters. 100 applications of the naive approach returned between 1,796 and 2,010 pairs, with a mean of 1,893.23 and a standard deviation of 34.29. GRAND finds 3,282 non-redundant pairs, which increases the non-redundant data by 63.3% over the maximum naive result and 73.4% over the mean.

GRAND offers a fast, standard process for creating non-redundant datasets that consistently contain more data than is achieved by a random approach, offering increases of between 23.6% and 73.4% more paired samples in the datasets to which we applied it.

2.2 CNN models can learn PPI prediction from non-redundant datasets

Knowing that out-of-network PPI prediction is a difficult task, we anticipated that finding the right model architecture to learn from our ArabidopsisPPI dataset would be important. We conducted a wide random search of the model hyperparameter space in which we varied which layers we used, and also parameters controlling the tightness of fit including dropout rate, regularisation parameters and CGR resolution.

We selected the structure for our CNN architecture using a random grid search of a wide parameter space. The structures followed the same pattern: the channels were split and passed through a convolutional stage consisting of zero or more “convolutional blocks” which each contained one or more convolutional layers. As in Hashemifar et al. (2018), we used a single model for this convolutional stage allowing a single set of model weights to be trained on both interacting partners’ sequences. As our CGR attractors are “image-like”, we examined well-known and well-performing models from the field of image processing as they were implemented in the Keras Python package, such as ResNet(He et al. 2015), EfficientNet(Tan and Le 2019) and VGG19(Simonyan and Zisserman 2014). Such models proved unsuitable for immediate use as the dimensions of our CGRs were too small for the models’ depth and convolutional size, but we took inspiration from the ResNet(He et al. 2015) architecture by incorporating potential “skip” layers within these convolutional blocks when they contained more than one layer; this structure has performed well for computer vision

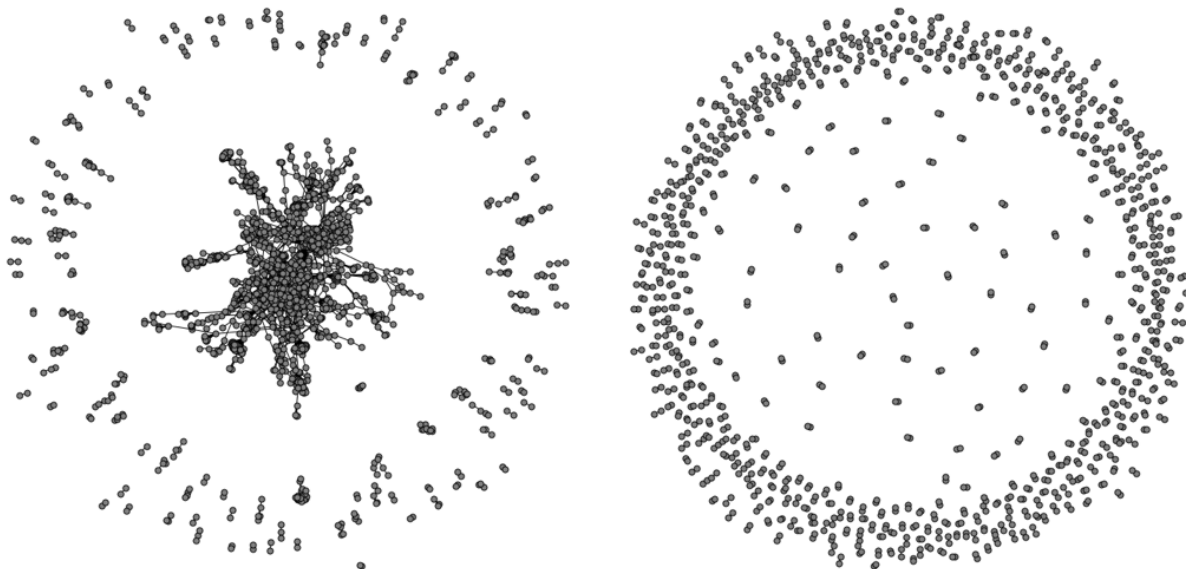


Figure 2: (a) The network of *Arabidopsis thaliana* PPIs from which the positive samples were selected. Nodes are clusters of similar genes, and edges represent a known interaction between one or more proteins. (b) The network after filtering with GRAND.

tasks, addressing the “vanishing gradient” issue. Following this convolutional stage the outputs for each input channel are pooled and concatenated to create a single vector for each sample. A dense stage follows, wherein the vector is passed through zero or more dense layers. A final classification layer with sigmoid activation provides the model’s output, and binary cross-entropy is used as the model’s loss function. We searched the space by varying the numbers and depths of these layers, convolutional filter sizes, dropout rates and regularisation parameters, as well as the choice of k which dictates the size and resolution of the initial input. For each value of k , the same 1,000 models were tested 5 times by training on 60% of the dataset, using a 20% split for validation purposes. The same 20% was withheld each time for final testing after the models trained and the final models were selected based on validation performance. Each model was trained for a maximum of 500 epochs, with early stopping triggered if the validation loss stopped improving, and a model checkpoint kept track of the version that achieved the best validation results.

The validation accuracy varied from around 50%, at which point the model is indistinguishable from random, up to 70.2%. The amount of models with poor validation performance may indicate the difficulty of generalisable learning in this task. We examined the relationships between various parameters and their results, such as the number of convolutional blocks as shown in Figure 3. We found that no models that skipped the convolutional stage were able to achieve above 65%, while the best results were obtained by models that included two or three convolutional blocks.

We also studied the effect of k on accuracy in our ResNet-inspired models. The results, as shown in Figure 4, show that the smaller, lower-resolution 4-mers yield better validation accuracy than higher values of k .

The top 25 models from the 4,000 models considered in the architecture search were carried forward to testing with the remaining 20% of the data. While these models achieved mean validation accuracies of up to 70.2% (see Figure 4), the highest mean accuracy achieved on the holdout data was 65.0%; through the use of an ensemble of different models compiled with a meta-learner, this was increased to 66.7%.

2.3 Alternatives to deep learning do not achieve comparable accuracy

To explore whether our deep learning approach was necessary, we applied two non-Neural Network machine learning methods, support vector classifiers and random forest classifiers, to the same *Arabidopsis*PPI dataset formatted as vectors of k -mer counts. In each case, we performed a grid search using training and validation splits to find the hyperparameters that achieved the highest validation accuracy, then applied those trained models to the 20% of samples that were held out for testing. Again, larger values of k yielded worse results; validation accuracies achieved using 5-mer, 6-mer and 7-mer counts appeared indistinguishable from random chance, ranging from 42.5% to 54.3%. The best results were achieved by the support vector classifier using a radial basis function kernel on vectors of 3-mers,

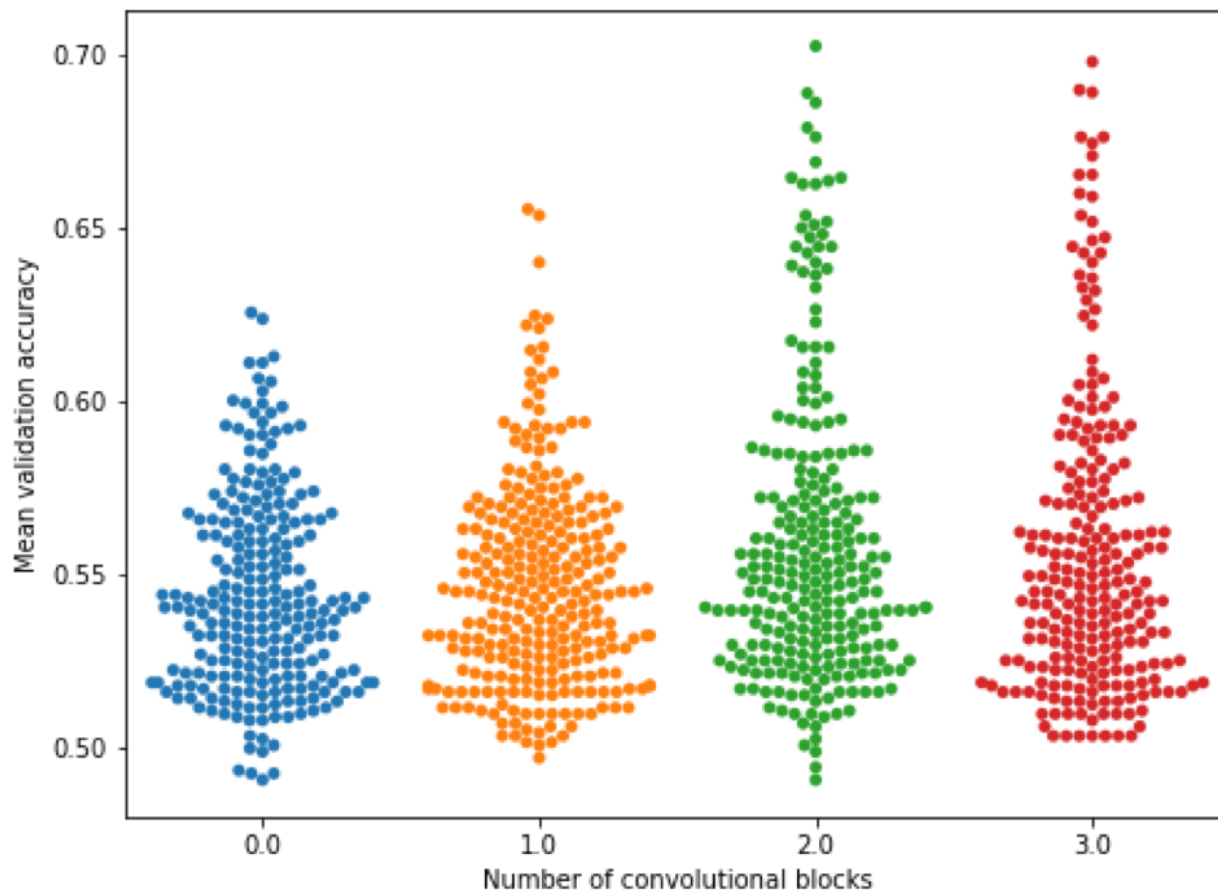


Figure 3: Mean validation accuracy from a ResNet random grid architecture search using a dataset of 4-mers, with increasing convolutional blocks

which reached a validation accuracy of 58.4%. However, this failed to generalise to the hold-out data as the test accuracy was 52.3%.

2.4 Transfer learning allowed modest learning from a related but very small dataset

We applied our methods to our EffectorPPI dataset in order to focus specifically on the interactions between R-Proteins and *Arabidopsis thaliana* proteins.

To begin, we repeated the hyperparameter search repeated using training and validation subsets taken from our EffectorPPI dataset. Some parameter sets appeared to perform well, with one model architecture achieving a mean validation accuracy of 73.9%. However, when the best of these models according to validation accuracy were applied to the holdout test data, they failed to achieve any test accuracy higher than 55.4%, close to the expected performance of a random classifier on the 50% positive, 50% negative data.

As this contains approximate one sixth of the number of samples in ArabidopsisPPI, we explored tactics for using what the models had previously learned from the comparatively abundant ArabidopsisPPI dataset. The first method used the results of the ArabidopsisPPI architecture, taking the hyperparameter sets that achieved the ten highest validation accuracy scores when trained and validated using ArabidopsisPPI. We then initialised these models with random weights and trained, validated and tested them on the EffectorPPI data. The best mean holdout accuracy obtained by one of these randomly initialised models was 0.576.

In our second approach, we used the same ten architectures found using the ArabidopsisPPI parameter search, but instead of randomly initialising new instances of these models, we used the five model checkpoints that were produced as each model was repeatedly trained with ArabidopsisPPI. These were used as the starting point for training and validating on subsets of EffectorPPI, and the highest achieved mean holdout accuracy was 60.0%.

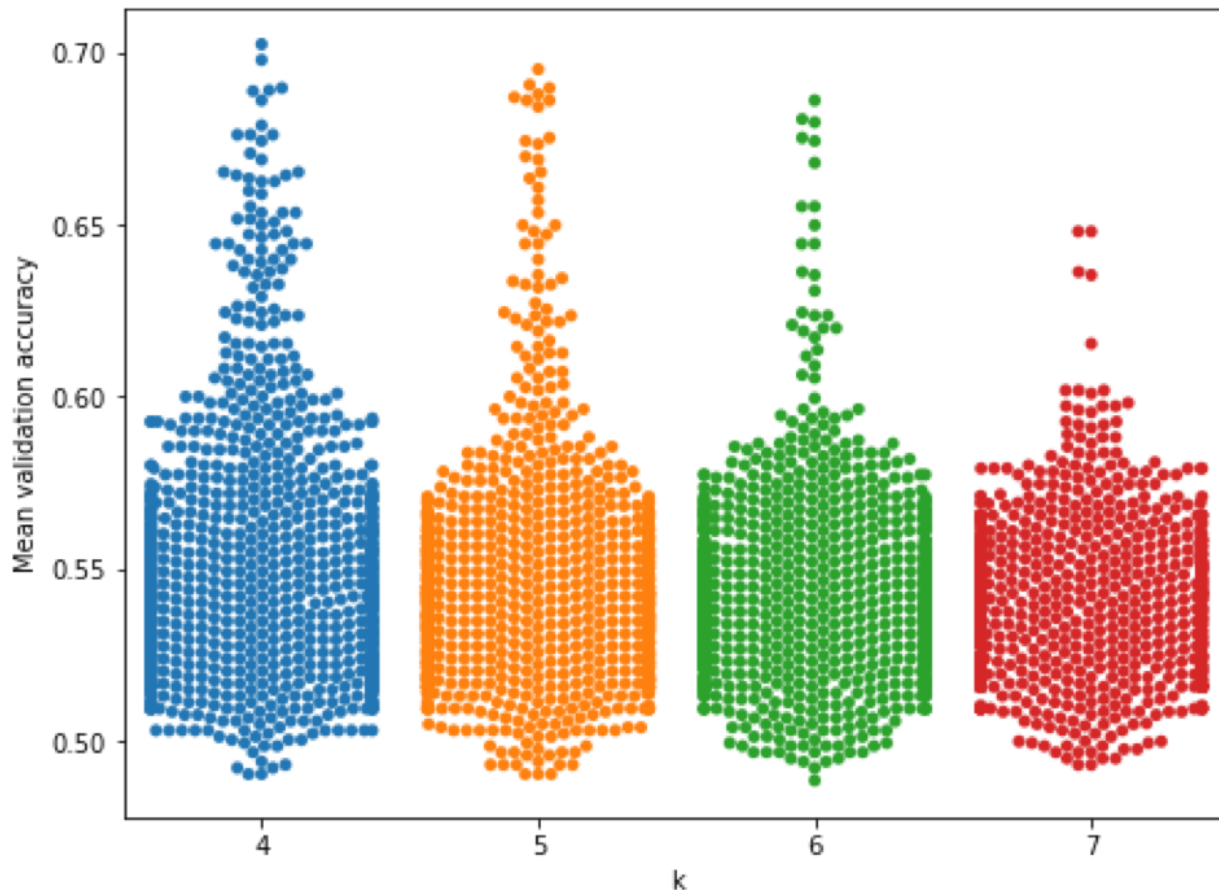


Figure 4: Mean validation accuracy from a random grid search of ResNet architectures across a range of k lengths

The final transfer learning approach we took used the same ten parameter sets, and again started with the model checkpoints trained on ArabidopsisPPI. We froze the weights in all but the final classification layer of each model, before retraining using the same subsets of EffectorPPI. The models trained in this manner achieved up to 0.597 test accuracy.

Across the top ten models by validation, the second approach (training on ArabidopsisPPI, then retraining all layers on EffectorPPI) yielded generally higher holdout results, outperforming the models trained from random initialisation for 6 of the 10 architectures, and outperforming the models where only the classification layer was retrained in 7 of the 10 cases. However, the performance ranking varied between architectures, and the single model with the most consistent good performance was trained using the weight-freezing approach; each of the holdout tests achieved an accuracy between 0.581 and 0.635.

2.5 The architecture extends to other data and achieves state-of-the-art results on difficult benchmark cases

Table 1: outperforms existing PPI papers

Model	Negatome	Recombine.pairs
Best published F1 score	0.87	0.68
Our F1 score (Ensemble)	0.90	0.79

We wanted to compare the models we had found with models in the existing literature by using a benchmark PPI dataset. Wei et al. (2017) provides a set of positive PPI pairs and three alternative sets of negative PPI pairs using different strategies. We used the positive data along with the Negatome negative data for one test and the positive data and the RecombinePairs negative data for another.

We found the best ensemble of 10 high-performing models according to the ArabidopsisPPI validation dataset and applied it to each dataset. Table 1 shows the F1 scores achieved by this ensemble on each set. Distinguishing between the positive data and Negatome negative data appears to be comparatively easy; the F1 scores published in Wei et al. (2017) reached 0.87, and our model performed similarly at 0.90. The RecombinePairs negative data provides a much more difficult challenge as the positive and negative data contain very similar samples. Some of the methods tested in Wei et al. (2017) obtained close to random performance, while they were able to achieve an F1 score of 0.68 with their highest-performing model. Our ensemble model achieved an F1 score of 0.79, which has not been surpassed as far as we could find among other works citing Wei et al. (2017). This suggests our model offers an improvement over previous methods of learning PPI prediction, particularly where the data is challenging to discriminate between.

2.6 Strategies for augmentations and synthetic data remain unsolved

We have exploited the image-like arrangement of k -mers in CGR attractors to develop model architectures inspired by research in the computer vision field. Our ResNet-inspired twinned architecture models were able to learn from non-redundant data and make predictions on out-of-network PPIs with state-of-the-art accuracy. However, the non-redundant datasets produced by GRAND are still comparably small by the standards of deep learning where benchmark sets like ImageNet(Deng et al. 2009) contain millions of training images. Typical computer vision methods for augmenting training data manipulate images in each training cycle, to increase the variety of training data seen by a model. These methods are not suited for application to CGR attractors as augmentation such as rotating, cropping, and recolouring CGR images would change the k -mer counts they represent, destroying the original biological sequence data. We explored two techniques to generate new data from samples in the ArabidopsisPPI training data. In the first method, synonymous substitution, we replace codons in the coding region of a gene sequence with other codons such that the produced protein still has the same sequence of amino acids. The second method uses generative deep learning to create CGR-like images.

2.6.1 Synonymous substitution produces CGRs with extremely likely labels, but does not improve model performance

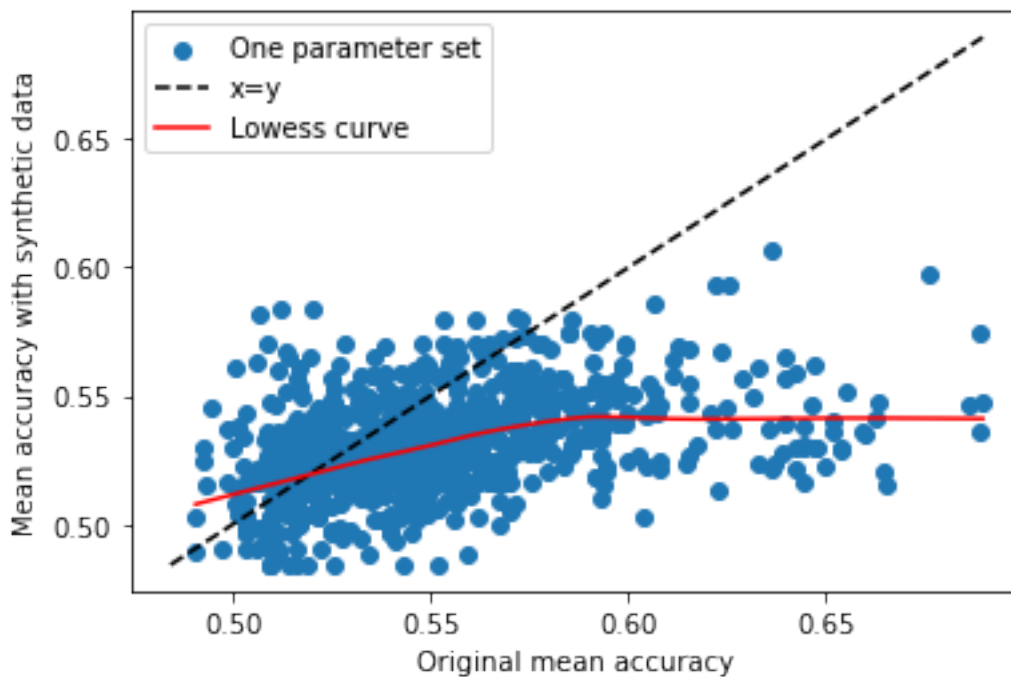


Figure 5: Scatter plot comparing validation accuracy achieved by each parameter set when trained on data with and without synthetic data generated by synonymous substitutions included in the training data.

We generated 10 synthetic samples for each real interaction pair in our ArabidopsisPPI 4-mers dataset using the synonymous substitution method, and trained and validation the same parameter sets with the synthetic training data included. As Figure 5 shows, the highest validation accuracies were achieved without the use of synthetic data. Fitting a Lowess curve elucidates this further: when the model originally performed essentially randomly, the synthetic data was in some cases able to raise the validation accuracy, but as the original performance improves the synthetic data

more often results in worse performance. Only 23.2% of models were more accurate with the addition of synthetic data, and the best validation accuracy achieved among these was only 0.61.

2.6.2 Conditional GANs models can produce CGRs that appear real, but reduce models' accuracy

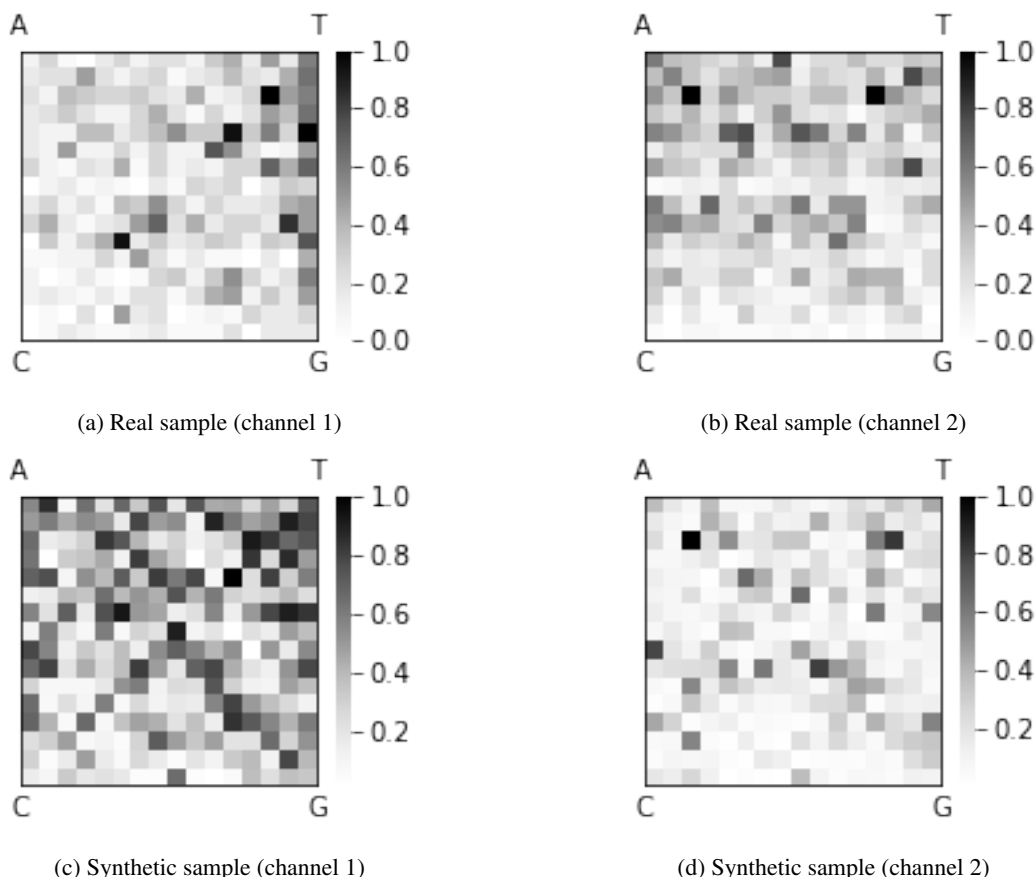


Figure 6: GAN outputs

Figure 6 shows real and synthetic CGR attractors. The real images (Figure 6a and Figure 6b) represent the two proteins interacting in a real PPI. The synthetic images (Figure 6c and Figure 6d) were generated using a cGAN model as examples of the true interacting class.

While the generated images appear similar to the real CGR attractors, they result in worse performance. We took the parameter sets that yielded the highest validation accuracy on the real ArabidopsisPPI dataset and retrained them with 2,000 true and 2,000 false synthetic samples included. Figure 7 plots the holdout accuracy, and shows that only three of the models performed marginally better with the synthetic data included.

2.7 CGRs contain k -mer count features that indicate taxonomic ranks, introducing potential bias

We continued the experiments into our approach to CGR-based PPI prediction by attempting to repeat the GRAND and architecture search processes using data taken from the HPIDB database (Ammari et al. 2016). At 3,282 non-redundant pairs, this set is larger than ArabidopsisPPI (1,106 pairs) and EffectorPPI (183 pairs). It also includes more variety among hosts; while EffectorPPI is limited to interactions between Arabidopsis thaliana and pathogens, HPIDB includes 66 host species.

Initial results were promising, with validation accuracy reaching 78.45%. However, we questioned whether we could be confident that the model was learning patterns relating to the actual interactions, or whether it was biased by species information. The positive samples experimentally validated interactions between hosts and pathogens from various species, whereas the negative data is randomly drawn from all hosts and all species. As our chosen CGR format represents the coding sequence that codes for a protein rather than the amino acid sequence, our data includes features that have been used in the field of metagenomics to characterise and distinguish genomes such as GC-content, codon usage and di-, tri- and tetranucleotide frequencies. While it is possible that the model may learn subtleties of interaction

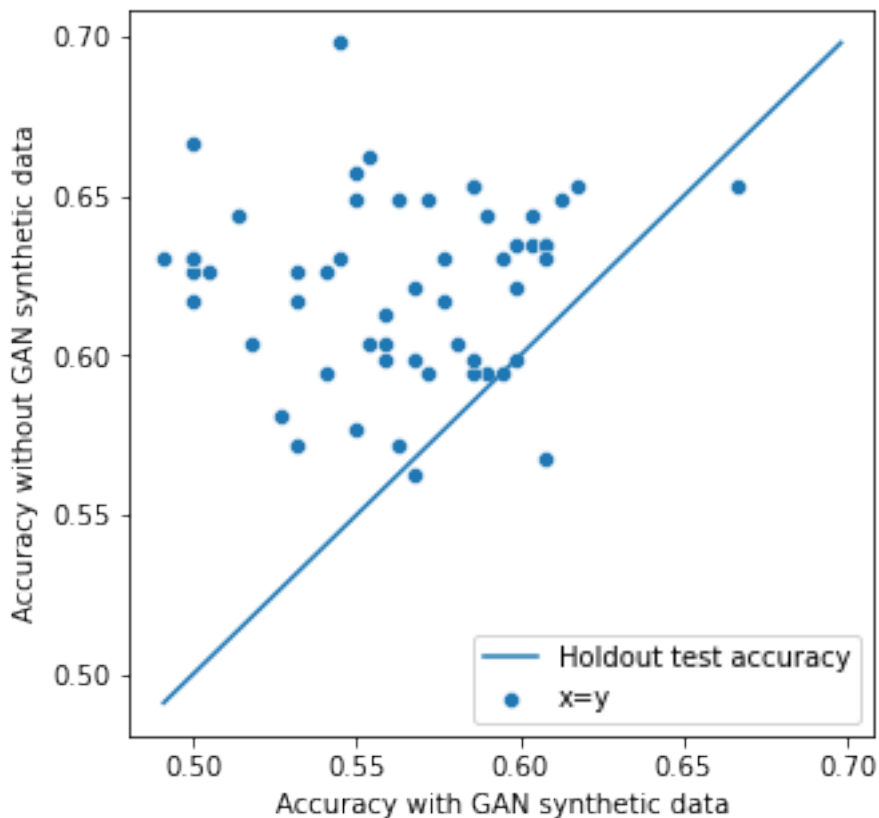


Figure 7: Scatter plot comparing holdout results from the best-performing models according to validation accuracy with and without the inclusion of GAN-generated synthetic images in the training data. A line marks where results would be equal.

that preclude, for example, an *Arabidopsis* R-protein interacting with an influenza effector, it may also have simply learned to reject the interaction because the host does not have the sequence characteristics of an animal.

To explore this hypothesis we masked our dataset, replacing each CGR with a one-hot encoding of the species from which the gene originated. We trained and tested a k-nearest neighbour classifier on the masked data and from the species alone, achieved a holdout test accuracy of 87.67%. This indicates that bias is present in the species distributions of the data, from which even a simple model can appear to learn to accurately predict interactions.

In order to learn from this bias, our models would have to be able to know from which species a gene represented in a CGR had originated. We therefore wanted to see if CGR attractors from different species' genomes were noticeably different. We compared the sequences of two different genomes, building CGR attractors for all CDS sequences in the *Magnaporthe oryzae* and *Oryza sativa* genomes as shown in Figure 8. We compiled all CGR attractors into a single image for each of the *Magnaporthe* (Figure 8b) and rice (Figure 8a) genomes. There are some visible differences for individual cells such as strong representation of individual 4-mers such as "CTCC" in *Oryza* and "CGAG" in *Magnaporthe*. There also appears to be a more general pattern, in that the *Oryza* CGR is strongest at certain positions along the A-G diagonal and C-G horizontal lines, and *Magnaporthe* is generally darker at most other points below the A-G diagonal. Figure 8c shows this pattern via a heatmap of the differences between the two plots where the scaled pathogen combined CGR was subtracted from the scaled host combined CGR.

2.8 CGR CNNs can learn to perform taxonomic classification

The HPIDB dataset bias and the differing features between genomes cast doubt on our intended goal of predicting the interactions in the HPIDB dataset. However, the ability to distinguish between taxonomic classes also has potential applications. We wanted to investigate whether CNNs trained with CGR attractors would work well at taxonomic classification tasks as, when built and trained, our resulting models could provide a relatively light-weight alternative to existing taxonomic classification models. We performed two experiments to this end. In the first, we classified

gene CGRs according to their superkingdom to see how well the model could give a broad overview of an unknown gene’s origin. In the second, we classified read CGRs according to whether they came from a specific host or pathogen organism, as this may be helpful as an early step in assembling sequences taken from sequencing an infected plant.

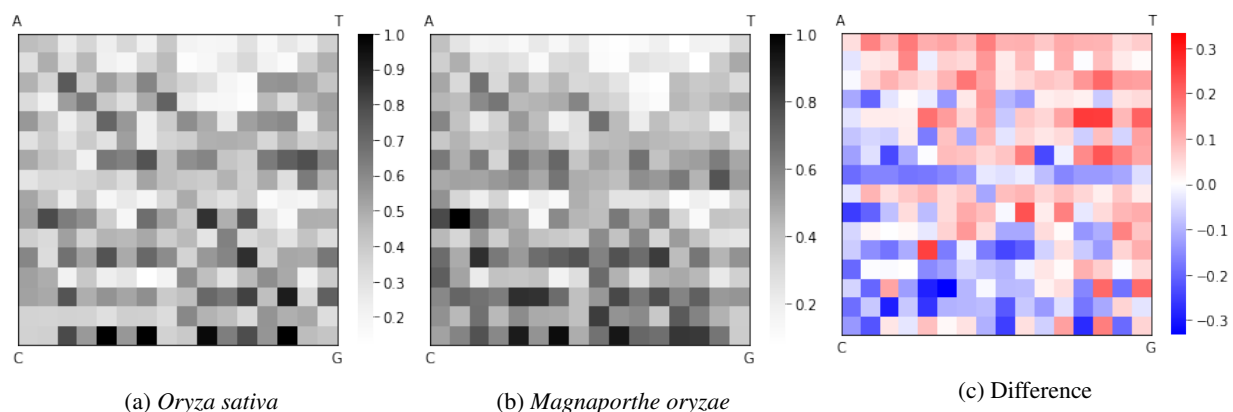


Figure 8: CGRs showing the entire genome for (a) a host (*Oryza sativa*) and (b) a pathogen (*Magnaporthe oryzae*) species, scaled to values between 0 and 1. (c) shows the difference between the two plots, where positive (red) values indicate that the 4-mer was more represented in the *Oryza sativa* genome and negative (blue) values indicate that the 4-mer was more represented in the *Magnaporthe oryzae* genome.

The best-performing model architectures found during the PPI prediction model search were not directly applicable to the classification problems due to differences in input and output of the tasks. We performed new parameter searches for each taxonomic classification task, where each model would take in one CGR as input, and output predictions of class membership.

Figure 9 shows the holdout test performance of a CNN trained on CGRs taken from our HPIDB dataset and labelled according to superkingdom. The mean class accuracy was 86.17%. The 757 bacteria samples in the test data were generally predicted well, with 94% correctly identified. There was some confusion between eukaryota and viruses; the model achieved class accuracies of 88% for the more abundant eukaryotic test samples and 77% for the viruses.

Read classifier results are shown in Figure 10. While the *Oryza sativa* reads were classified correctly in 94.3% of cases, the prediction of *Magnaporthe oryzae* reads were only correct in 60.4% of reads tested, giving a mean class accuracy of 77.37%. While the model did learn to discriminate between the two classes to a degree, the use of CGRs and a CNN did not seem to achieve more than is possible without them. We trained a linear logistic regression model on the same data, extracting the k -mer counts from the CGR attractors into feature vectors. It performed similarly with a mean class accuracy of 76.90%, where the model was better at classifying the *Oryza* reads.

3 Discussion

The task of PPI prediction is challenging, and machine learning approaches require careful consideration of the data that is used. Machine learning requires abundant data but including all known interactions introduces representation bias. However, the interactions in PPI datasets often consist of many interactions for the same proteins, so eliminating redundancy significantly reduces the amount of available data. We have developed an algorithm for eliminating redundant data while maintaining more samples than random discarding.

From a comprehensive architecture search we have developed a model that is able to learn PPI prediction from small, non-redundant datasets. When applied to the benchmark PPIPre datasets, we obtained results higher than previously achieved for both the easier Negatome version and the difficult RecombinePairs version of the data.

Smaller values of k result in better prediction accuracy despite the coarser resolution information they contain. It may be that shorter sequences are sufficient to discriminate between classes making longer sequences redundant. It may also be that as the CGRs double in height and width with each increment of k , larger attractors contain too many more features than there are samples in the dataset, resulting in more overfitting. Finally, higher values of k mean that there are more possible k -mers, and so fewer cells in a CGR will contain data. CNN models are known to perform badly on sparse data.

The arrangement of k -mer counts within CGRs has assisted with this performance, as subsets of the search area that do not include convolutional layers do not obtain the same maximum accuracy. Furthermore, machine learning methods

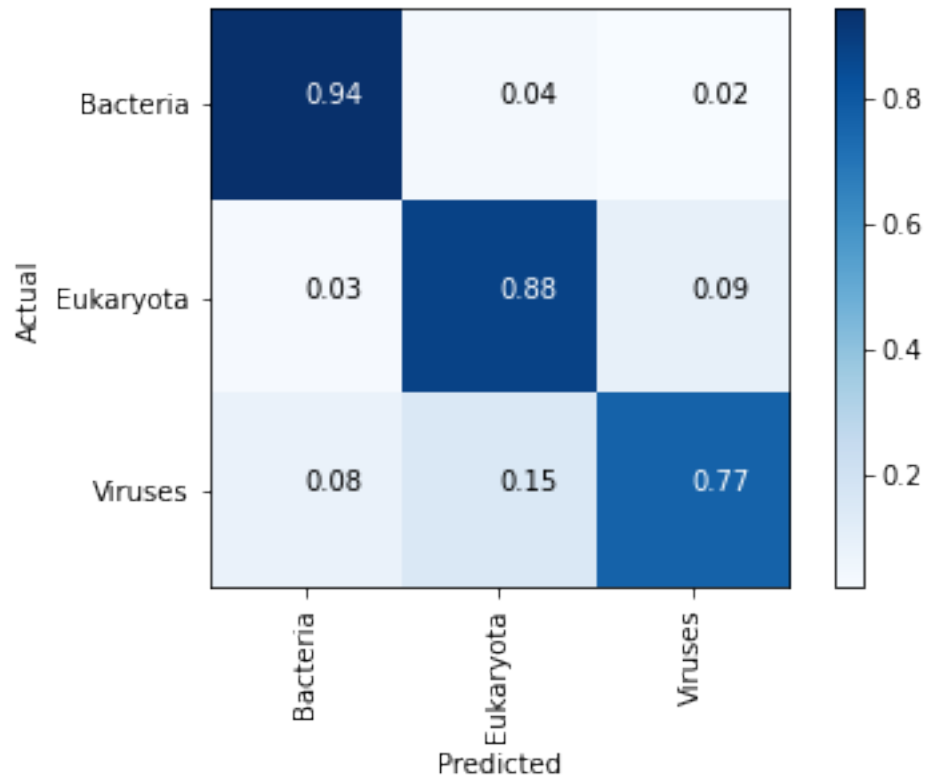


Figure 9: Confusion matrix from a CNN model which uses CGR inputs to predict super kingdom from CDS region. Data was extracted from the HPIDB dataset and consists of 757 bacteria samples, 1,745 eukaryote samples and 124 virus samples

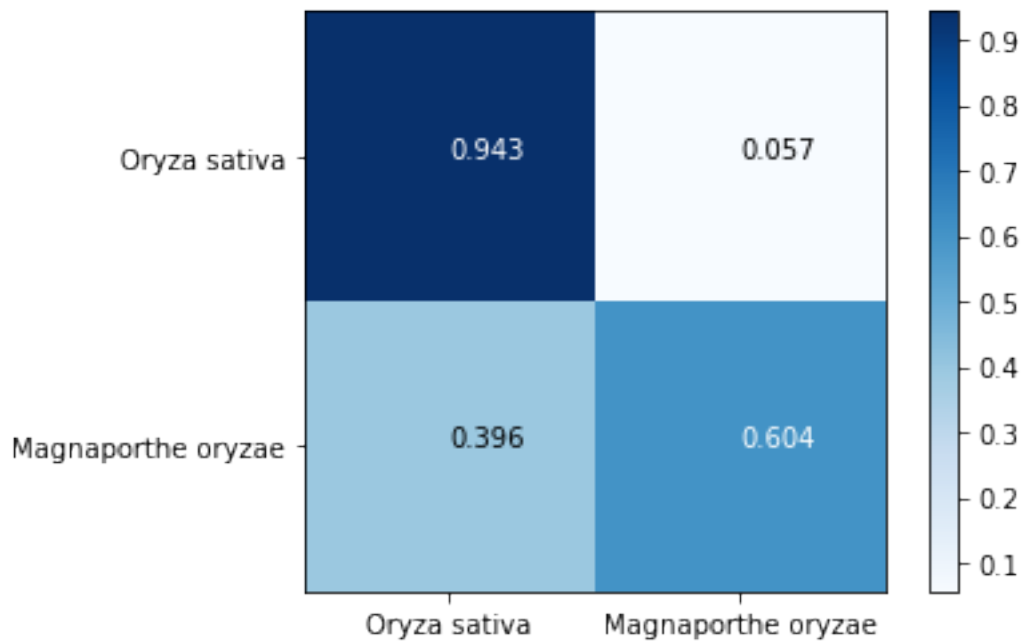


Figure 10: Confusion matrix showing the results of a CNN model attempting to classify synthetic reads

without neural networks that use vectors of k -mer counts as their input without regard to order do not perform as well as the CGR CNN models. Whether there are different arrangements within a CGR-like structure that would lead to higher performance remains an open question.

We explored a method of augmenting a CGR dataset with synthetic sequences by synonymous substitution, theorising that as the different CDS sequences would encode the same protein sequence, homology and likely identical behaviour would follow. While augmenting images to increase the variety of input often increases the accuracy of computer vision models, our experiments showed that this means of augmentation generally does not improve our model at its PPI prediction task. The synonymous substitutions appear to offer some improvement when the model performed particularly badly on the validation data without augmented training data. We consider that this may be the result of a slight reduction in overfitting that caused the original poor performance. However, the improvements gained by adding the synthetic images were much weaker than improvements gained by choosing more suitable architecture, and when performance was high without synonymous substitutions, their addition made validation accuracy worse. We also note that depending on the intended task of the model, the substitutions may lose codon usage or tetranucleotide frequency biases that may have been useful features.

GANs do not provide even this small potential for improvement, but almost always worsened performance. The GAN model itself may require more data in order to learn enough to produce synthetic images with sufficient accuracy and variety. It may also be the case that while the generated CGR attractors seem to share qualities with the real images to the human eye, they lack important distinguishing features needed for class distinction.

The question of suitable augmentations for deep learning of genetic data therefore remains open.

We have also shown that machine learning methods using k -mer counts to predict protein-protein interactions could introduce bias if positive and negative samples use different species pairings. k -mer counts can be sufficient to identify taxonomic classifications, and uneven species pairings between positive and negative data can be sufficient to separate the data. Our models for high-level taxonomic classification were able to learn features to discriminate between genomes with accuracy that is high, albeit not comparable with existing weightier methods. In addition, linear logistic regression using k -mer counts achieved similar performance, indicating that for these tasks the CGR arrangement and CNN architecture do not contribute to learning. Dick and Green (2020)'s comprehensive study uses several approaches to building CGRs from proteins, building models to identify the source organisms of protein source identification. While their predictions were better than random chance, they described these results as "modest". Our taxonomic experiments, which look at broader classes, are not directly comparable but generally perform well and achieve >90% accuracy in the prediction of some classes. Our CGRs, and the k -mers we use for logistic regression, are built with the benefit of the true knowledge of the genetic coding sequence, which may underline the importance of features such as nucleotide pattern frequency and codon usage in taxonomic classification tasks, and the relative difficulty of identifying source organism from protein sequence and from genetic sequence.

To COVID. Which made this all a lot more fiddly than it needed be.

We would like to thank George Deeks and the Norwich Bioscience Institutes' Research Computing department for their assistance with the High Performance Computing cluster. We would also like to thank Volodymyr Chapman for compiling the ArabidopsisPPI data, Anthony Duncan for helpful discussions about metagenomics and Bethany Nichols for naming GRAND. RV was supported by BBSRC grant number BB/V509267/1. This work was supported by Wave 1 of The UKRI Strategic Priorities Fund under the EPSRC Grant EP/T001569/1, particularly the "AI for Science" theme within that grant & The Alan Turing Institute. DM was supported by The Gatsby Charitable Foundation through a core grant to The Sainsbury Laboratory.

References

- Abbas, Amreen, Sweta Jain, Mahesh Gour, and Swetha Vankudothu. 2021. "Tomato Plant Disease Detection Using Transfer Learning with c-GAN Synthetic Images." *Computers and Electronics in Agriculture* 187: 106279. <https://doi.org/https://doi.org/10.1016/j.compag.2021.106279>.
- Albert, Paul, Mohamed Saadeldin, Badri Narayanan, Brian Mac Namee, Deirdre Hennessy, Aisling O'Connor, Noel O'Connor, and Kevin McGuinness. 2021. "Semi-Supervised Dry Herbage Mass Estimation Using Automatic Data and Synthetic Images." In *Proceedings of the IEEE/CVF International Conference on Computer Vision (ICCV) Workshops*, 1284–93.
- Ammari, Mais G., Cathy R. Gresham, Fiona M. McCarthy, and Bindu Nanduri. 2016. "HPIDB 2.0: a curated database for host–pathogen interactions." *Database* 2016 (July). <https://doi.org/10.1093/database/baw103>.
- Berardini, Tanya Z, Leonore Reiser, Donghui Li, Yarik Mezheritsky, Robert Muller, Emily Strait, and Eva Huala. 2015. "The Arabidopsis Information Resource: Making and Mining the 'Gold Standard' Annotated Reference Plant Genome." *Genesis* 53 (8): 474–85.

- Bromley, Jane, Isabelle Guyon, Yann LeCun, Eduard Säckinger, and Roopak Shah. 1993. "Signature Verification Using a Siamese Time Delay Neural Network." *Advances in Neural Information Processing Systems* 6.
- Deng, Jia, Wei Dong, Richard Socher, Li-Jia Li, Kai Li, and Li Fei-Fei. 2009. "Imagenet: A Large-Scale Hierarchical Image Database." In *2009 IEEE Conference on Computer Vision and Pattern Recognition*, 248–55. Ieee.
- Deschavanne, P, and P Tuffery. 2008. "Exploring an Alignment Free Approach for Protein Classification and Structural Class Prediction." *Biochimie* 90 (4): 615–25.
- Dick, Kevin, and James R Green. 2020. "Chaos Game Representations & Deep Learning for Proteome-Wide Protein Prediction." In *2020 IEEE 20th International Conference on Bioinformatics and Bioengineering (BIBE)*, 115–21. IEEE.
- Ding, Ziyun, and Daisuke Kihara. 2019. "Computational Identification of Protein-Protein Interactions in Model Plant Proteomes." *Scientific Reports* 9 (1): 1–13.
- Dwibedi, Debidatta, Ishan Misra, and Martial Hebert. 2017. "Cut, Paste and Learn: Surprisingly Easy Synthesis for Instance Detection." In *Proceedings of the IEEE International Conference on Computer Vision*, 1301–10.
- Eid, Fatma-Elzahraa, Haitham A Elmarakeby, Yujia Alina Chan, Nadine Fornelos, Mahmoud ElHefnawi, Eliezer M Van Allen, Lenwood S Heath, and Kasper Lage. 2021. "Systematic Auditing Is Essential to Debiasing Machine Learning in Biology." *Communications Biology* 4 (1): 183.
- Epic Games. 2023. "Unreal Engine." <https://www.unrealengine.com>.
- Evans, Richard, Michael O'Neill, Alexander Pritzel, Natasha Antropova, Andrew Senior, Tim Green, Augustin Zidek, et al. 2021. "Protein Complex Prediction with AlphaFold-Multimer." *bioRxiv*. <https://doi.org/10.1101/2021.10.04.463034>.
- Franceschetti, Marina, Abbas Maqbool, Maximiliano J Jiménez-Dalmaroni, Helen G Pennington, Sophien Kamoun, and Mark J Banfield. 2017. "Effectors of Filamentous Plant Pathogens: Commonalities amid Diversity." *Microbiology and Molecular Biology Reviews : MMBR* 81 (2): e00066–16. <https://doi.org/10.1128/MMBR.00066-16>.
- González-Fuente, Manuel, Sébastien Carrère, Dario Monachello, Benjamin G Marsella, Anne-Claire Cazalé, Claudine Zischek, Raka M Mitra, et al. 2020. "EffectorK, a Comprehensive Resource to Mine for Ralstonia, Xanthomonas, and Other Published Effector Interactors in the Arabidopsis Proteome." *Molecular Plant Pathology* 21 (10): 1257–70.
- Goodfellow, Ian, Jean Pouget-Abadie, Mehdi Mirza, Bing Xu, David Warde-Farley, Sherjil Ozair, Aaron Courville, and Yoshua Bengio. 2014. "Generative Adversarial Nets." In *Advances in Neural Information Processing Systems*, edited by Z. Ghahramani, M. Welling, C. Cortes, N. Lawrence, and K. Q. Weinberger. Vol. 27. Curran Associates, Inc. <https://proceedings.neurips.cc/paper/2014/file/5ca3e9b122f61f8f06494c97b1afccf3-Paper.pdf>.
- Haas, Brian J, Sophien Kamoun, Michael C Zody, Rays HY Jiang, Robert E Handsaker, Liliana M Cano, Manfred Grabherr, et al. 2009. "Genome sequence and analysis of the Irish potato famine pathogen *Phytophthora infestans*." *Nature* 461 (7262): 393–98. <https://doi.org/doi:10.1038/nature08358>.
- Hamp, Tobias, and Burkhard Rost. 2015. "More Challenges for Machine-Learning Protein Interactions." *Bioinformatics* 31 (10): 1521–25.
- Hashemifar, Somaye, Behnam Neyshabur, Aly A Khan, and Jinbo Xu. 2018. "Predicting Protein-Protein Interactions Through Sequence-Based Deep Learning." *Bioinformatics* 34 (17): i802–10.
- He, Kaiming, Xiangyu Zhang, Shaoqing Ren, and Jian Sun. 2015. "Deep Residual Learning for Image Recognition." *arXiv*. <https://doi.org/10.48550/ARXIV.1512.03385>.
- Huang, Weichun, Leping Li, Jason R. Myers, and Gabor T. Marth. 2011. "ART: a next-generation sequencing read simulator." *Bioinformatics* 28 (4): 593–94. <https://doi.org/10.1093/bioinformatics/btr708>.
- Jeffrey, H Joel. 1990. "Chaos Game Representation of Gene Structure." *Nucleic Acids Research* 18 (8): 2163–70. <https://doi.org/https://10.1093/nar/18.8.2163>.
- Jia, Jianhua, Xiaoyan Li, Wangren Qiu, Xuan Xiao, and Kuo-Chen Chou. 2019. "iPPI-PseAAC (CGR): Identify Protein-Protein Interactions by Incorporating Chaos Game Representation into PseAAC." *Journal of Theoretical Biology* 460: 195–203.
- Jones, David T. 2019. "Setting the Standards for Machine Learning in Biology." *Nature Reviews Molecular Cell Biology* 20 (11): 659–60.
- Jumper, John, Richard Evans, Alexander Pritzel, Tim Green, Michael Figurnov, Olaf Ronneberger, Kathryn Tunyasuvunakool, et al. 2021. "Highly Accurate Protein Structure Prediction with AlphaFold." *Nature* 596 (7873): 583–89.
- Krishnakumar, Vivek, Matthew R. Hanlon, Sergio Contrino, Erik S. Ferlanti, Svetlana Karamycheva, Maria Kim, Benjamin D. Rosen, et al. 2014. "Araport: the Arabidopsis Information Portal." *Nucleic Acids Research* 43 (D1): D1003–9. <https://doi.org/10.1093/nar/gku1200>.
- Kristianingsih, Ruth, and Dan MacLean. 2021. "Accurate Plant Pathogen Effector Protein Classification Ab Initio with Deepredef: An Ensemble of Convolutional Neural Networks." *BMC Bioinformatics* 22 (1): 1–22.
- Kumar, Ranjit, and Bindu Nanduri. 2010. "HPIDB-a Unified Resource for Host-Pathogen Interactions." In *BMC Bioinformatics*, 11:1–6. 6. BioMed Central.

- Le, Quoc, and Tomas Mikolov. 2014. “Distributed Representations of Sentences and Documents.” In *International Conference on Machine Learning*, 1188–96. PMLR.
- Li, Weizhong, and Adam Godzik. 2006. “Cd-Hit: A Fast Program for Clustering and Comparing Large Sets of Protein or Nucleotide Sequences.” *Bioinformatics* 22 (13): 1658–59.
- Löchel, Hannah F, Dominic Eger, Theodor Sperlea, and Dominik Heider. 2020. “Deep Learning on Chaos Game Representation for Proteins.” *Bioinformatics* 36 (1): 272–79.
- Man, Keith, and Javan Chahl. 2022. “A Review of Synthetic Image Data and Its Use in Computer Vision.” *Journal of Imaging* 8 (11): 310.
- Mirza, Mehdi, and Simon Osindero. 2014. “Conditional Generative Adversarial Nets.” *arXiv Preprint arXiv:1411.1784*.
- Nalley, Lawton, Francis Tsiboe, Alvaro Durand-Morat, Aaron Shew, and Greg Thoma. 2016. “Economic and Environmental Impact of Rice Blast Pathogen (*Magnaporthe oryzae*) Alleviation in the United States.” *PLoS ONE* 11 (12): e0167295. <https://doi.org/10.1371/journal.pone.0167295>.
- Park, Yungki, and Edward M Marcotte. 2012. “Flaws in Evaluation Schemes for Pair-Input Computational Predictions.” *Nature Methods* 9 (12): 1134–36.
- Qiu, Jiajun, Michael Bernhofer, Michael Heinzinger, Sofie Kemper, Tomas Norambuena, Francisco Melo, and Burkhard Rost. 2020. “ProNA2020 Predicts Protein–DNA, Protein–RNA, and Protein–Protein Binding Proteins and Residues from Sequence.” *Journal of Molecular Biology* 432 (7): 2428–43. <https://doi.org/https://doi.org/10.1016/j.jmb.2020.02.026>.
- Rao, Roshan M, Jason Liu, Robert Verkuil, Joshua Meier, John Canny, Pieter Abbeel, Tom Sercu, and Alexander Rives. 2021. “MSA Transformer.” In *Proceedings of the 38th International Conference on Machine Learning*, edited by Marina Meila and Tong Zhang, 139:8844–56. Proceedings of Machine Learning Research. PMLR. <https://proceedings.mlr.press/v139/rao21a.html>.
- Rives, Alexander, Joshua Meier, Tom Sercu, Siddharth Goyal, Zeming Lin, Jason Liu, Demi Guo, et al. 2021. “Biological Structure and Function Emerge from Scaling Unsupervised Learning to 250 Million Protein Sequences.” *Proceedings of the National Academy of Sciences* 118 (15): e2016239118.
- Rockstar Games. 2013. “Grand Theft Auto v.”
- Rost, Burkhard. 1999. “Twilight Zone of Protein Sequence Alignments.” *Protein Engineering* 12 (2): 85–94.
- Saleh, Fatemeh Sadat, Mohammad Sadegh Aliakbarian, Mathieu Salzmann, Lars Petersson, and Jose M Alvarez. 2018. “Effective Use of Synthetic Data for Urban Scene Semantic Segmentation.” In *Proceedings of the European Conference on Computer Vision (ECCV)*, 84–100.
- Shin, Hoo-Chang, Neil A Tenenholz, Jameson K Rogers, Christopher G Schwarz, Matthew L Senjem, Jeffrey L Gunter, Katherine P Andriole, and Mark Michalski. 2018. “Medical Image Synthesis for Data Augmentation and Anonymization Using Generative Adversarial Networks.” In *Simulation and Synthesis in Medical Imaging: Third International Workshop, SASHIMI 2018, Held in Conjunction with MICCAI 2018, Granada, Spain, September 16, 2018, Proceedings 3*, 1–11. Springer.
- Simonyan, Karen, and Andrew Zisserman. 2014. “Very Deep Convolutional Networks for Large-Scale Image Recognition.” *arXiv*. <https://doi.org/10.48550/ARXIV.1409.1556>.
- Singh, Jaswinder, Jack Hanson, Kuldip Paliwal, and Yaoqi Zhou. 2019. “RNA Secondary Structure Prediction Using an Ensemble of Two-Dimensional Deep Neural Networks and Transfer Learning.” *Nature Communications* 10 (1): 5407.
- Sperschneider, Jana, Peter N Dodds, Donald M Gardiner, John M Manners, Karam B Singh, and Jennifer M Taylor. 2015. “Advances and challenges in computational prediction of effectors from plant pathogenic fungi.” *PLoS Pathogens* 11 (5): e1004806. <https://doi.org/10.1371/journal.ppat.1004806>.
- Tan, Mingxing, and Quoc V. Le. 2019. “EfficientNet: Rethinking Model Scaling for Convolutional Neural Networks.” <https://doi.org/10.48550/ARXIV.1905.11946>.
- Wang, Lei, Hai-Feng Wang, San-Rong Liu, Xin Yan, and Ke-Jian Song. 2019. “Predicting Protein-Protein Interactions from Matrix-Based Protein Sequence Using Convolution Neural Network and Feature-Selective Rotation Forest.” *Scientific Reports* 9 (1): 9848.
- Ward, Daniel, and Peyman Moghadam. 2020. “Scalable Learning for Bridging the Species Gap in Image-Based Plant Phenotyping.” *Computer Vision and Image Understanding* 197-198: 103009. <https://doi.org/https://doi.org/10.1016/j.cviu.2020.103009>.
- Wei, Leyi, Pengwei Xing, Jiancang Zeng, JinXiu Chen, Ran Su, and Fei Guo. 2017. “Improved Prediction of Protein–Protein Interactions Using Novel Negative Samples, Features, and an Ensemble Classifier.” *Artificial Intelligence in Medicine* 83: 67–74.
- Xu, Mingle, Sook Yoon, Alvaro Fuentes, and Dong Sun Park. 2023. “A Comprehensive Survey of Image Augmentation Techniques for Deep Learning.” *Pattern Recognition*, 109347.
- Yang, Shiping, Hong Li, Huaqin He, Yuan Zhou, and Ziding Zhang. 2019. “Critical Assessment and Performance Improvement of Plant–Pathogen Protein–Protein Interaction Prediction Methods.” *Briefings in Bioinformatics* 20 (1): 274–87.

- Yang, Xiaodi, Shiping Yang, Qinmengge Li, Stefan Wuchty, and Ziding Zhang. 2020. “Prediction of Human-Virus Protein-Protein Interactions Through a Sequence Embedding-Based Machine Learning Method.” *Computational and Structural Biotechnology Journal* 18: 153–61.
- Yu, Dingquan, Grzegorz Chojnowski, Maria Rosenthal, and Jan Kosinski. 2022. “AlphaPulldown—a python package for protein–protein interaction screens using AlphaFold-Multimer.” *Bioinformatics* 39 (1). <https://doi.org/10.1093/bioinformatics/btac749>.
- Yuliar, Yanetri Asi Nion, and Koki Toyota. 2015. “Recent trends in control methods for bacterial wilt diseases caused by *Ralstonia solanacearum*.” *Microbes and Environments* 30 (1): 1–11. <https://doi.org/10.1264/jsme2.ME14144>.

4 Appendix

5 Research Methods

5.1 Dataset preparation

We have presented results from PPI prediction experiments using two datasets, which we refer to as ArabidopsisPPI and EffectorPPI.

We built the larger dataset, ArabidopsisPPI, from 4,493 interactions between between *Arabidopsis thaliana* proteins. We restricted these to the interactions that are supported by direct evidence from TAIR(Berardini et al. 2015) and Araport(Krishnakumar et al. 2014).

The smaller dataset, EffectorPPI, focuses on interactions between *Arabidopsis thaliana* proteins and pathogen effectors. We extracted this data from the EffectorK(González-Fuente et al. 2020) collection of curated interactions.

We created a third dataset from interactions extracted from the Host-Pathogen Interaction Database (HPIDB)(Kumar and Nanduri 2010), which we intended to use for PPI prediction. After discovering that it was potentially biased, we instead extracted the CGRs from it to investigate taxonomic classification.

We made each of these collections of PPIs into CGR datasets using the same process. After filtering for redundancy using GRAND, we generated negative samples by pairing genes that were not selected for inclusion. We drew pairs of genes at random from these unused sequences, and then searched the original unfiltered data to ensure that there is no known interaction between these two genes or any other genes with similar sequences; sequences are considered similar if they have a nucleotide sequence identity of 80% or higher.

From the PPI data, we retrieve the CDS that encodes each protein and built these into CGR attractors using k -mers with lengths 4 to 7. We stack the attractors for each pair to create data with two channels.

5.2 GRAND

We applied GRAND to three datasets: ArabidopsisPPI, EffectorPPI, and the host-pathogen interactions taken from the HPIDB. The process followed was the same in each case.

Using the CD-Hit-Est program, we filtered CDS data to an 80% nucleotide sequence identity, which was the lowest threshold provided by the software. This resulted in clusters of similar sequences. We built a network graph, wherein nodes represented each CD-Hit cluster and edges represented that there was at least one known PPI between proteins coded for by sequences in the connected clusters. We then reduced the graph until it was non-redundant. While nodes existed that had only one neighbour, we would randomly select from them and find their one neighbour, removing all of that neighbours’ other edges. If there were no such nodes but there were still nodes with degree higher than one, we iterate across edges and, for each edge, take the sum of the degrees of the connected nodes. Nodes that have degree 0 are removed. This process continues until all remaining nodes have exactly degree one.

We generated negative samples by selecting pairs of remaining clusters and, provided that there was no known PPI interaction between proteins in the clusters, drew one sample at random from each cluster. The order of the proteins in the ArabidopsisPPI pairs was not relevant, so clusters were drawn at random. We drew host and pathogen clusters separately when generating negative data for the the HPIDB and EffectorK datasets to maintain a similar distribution of species within the negative data as the positive data.

5.3 Model architecture

Architectures were implemented, trained and tested in Python 3.6, using the Keras 2.2.4 and TensorFlow 1.11.0 libraries.

We explored parameter sets that varied details of the architecture and of the optimization. For k values 4,5,6 and 7, we tested 1,000 parameter sets. Optimizer details consisted of the optimization algorithm, learning rate and regularization parameters L1 and L2. Architecture parameters controlled the presence or absence of three main blocks and, where present, their number and shapes: the twinned ResNet block(s) each input was passed through; a second round of

ResNet blocks after concatenation of the paired inputs; dense layers before the final classification. Dropouts, filter widths and biases for each of the three main blocks were also included.

5.4 Ensembling method

We began by compiling validation results from all models tested in the ArabidopsisPPI parameter search. We took the top 25 parameter sets according to validation accuracy and created each combination of up to 10 of these models. For each combination, we loaded each model's checkpoint and found its classification of each sample in the validation data. We assigned these validation samples a predicted class by taking the individual models' predictions as votes.

5.5 Transfer learning

We applied four approaches to architecture selection and training for the EffectorPPI 4-mer dataset. A search for a parameter set was performed using EffectorPPI, finding the best-performing according to validation accuracy. The remaining three methods all used the best ten parameter sets according to the validation results on the larger ArabidopsisPPI dataset, but trained in different ways: training on EffectorPPI from a random initialisation; training initially on ArabidopsisPPI and then training further on EffectorPPI; training initially on ArabidopsisPPI, freezing all weights but those in the final classification layer and then training this layer on EffectorPPI.

5.6 Synthetic images

5.6.1 Synonymous substitutions

We used synonymous substitutions of nucleotides to generate new sequences from existing pairs of interacting proteins. We would build a new pair of sequences by iterating through both sequences, taking each codon in turn and randomly selecting from all codons that code for the same amino acid.

5.6.2 Generative Adversarial Nets

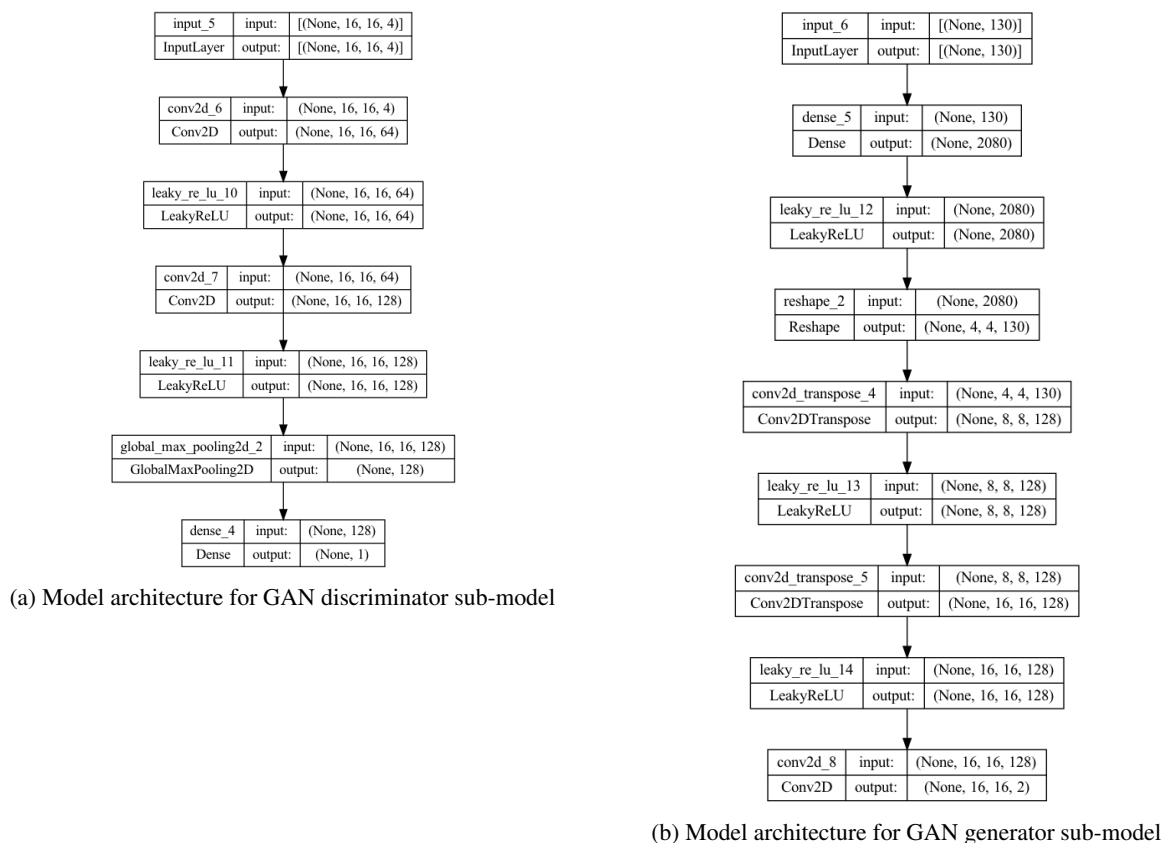


Figure 11: GAN architecture

We implemented a simple cGAN architecture in TensorFlow and Keras, following Keras' example of a cGAN model for generating MNIST digits. The generator model takes the structure shown in Figure 11b, and the discriminator model architecture is shown in Figure 11a. Both sub-models were trained with the Adam optimizer with beta parameters set

to 0.5. The learning rate for the generator was 3×10^{-4} , for the discriminator this was 3×10^{-3} . Hyperparameters were chosen by the researchers based on visual appearance; inappropriate hyperparameters led to images that either were clearly lacking the characteristics of CGRs or were almost identical within each class. All hyperparameters were chosen before the synthetic data was tested on the ArabidopsisPPI classification task. The GAN model was trained on ArabidopsisPPI for 200 epochs, and then for short bursts of 10 epochs at a time in between the generation of batches of fake images to further encourage diversity among images of the same class.

5.7 Taxonomic classification

5.7.1 Classification of taxonomic superkingdom

We took host-pathogen interactions from the HPIDB version 3.0 dataset (Kumar and Nanduri 2010) (Ammari et al. 2016) and reduced them to 3,282 non-redundant paired samples using GRAND. We paired each CGR with a one-hot encoding of the superkingdom of the organism from which the gene originated. As this data now has a single channel, we simplified the model architecture search space and performed validation testing for 100 randomly generated parameter sets. Each parameter set was tested 5 times. The set with the highest mean validation categorical accuracy used the architecture shown in Figure 12, was optimized using Adam with a learning rate of 0.001, and was then evaluated on the holdout data.

5.7.2 Host/pathogen read classification

We took all 12,755 and 42,355 CDS sequences from the *Magnaporthe oryzae* and *Oryza sativa* genomes respectively and created a training dataset of CGR attractors. We also created a test dataset using the ART software (Huang et al. 2011) to simulate Illumina single-end sequencing reads, resulting in 107,272 *Magnaporthe* and 259,361 *Oryza* reads. Variants of the CNN used for PPI prediction, using a single ResNet segment instead of a twinned structure, were trained on the CDS sequences and validated on synthetic reads represented as CGR attractors with class weighting applied during training. The model with the highest validation accuracy was then tested on the remaining synthetic reads' CGRs. This model, which used 5-mers, is shown in Figure 13. The hyperparameter search also included optimization parameters; the selected parameter set used the SGD optimizer with a learning rate of 1.5×10^{-3} . L1 and L2 regularisation were applied at rates 1×10^{-5} and 1×10^{-3} .

6 Online Resources

Code is available from https://github.com/TeamMacLean/GRAND_Code, and data is hosted at <https://zenodo.org/doi/10.5281/zenodo.10025321>.

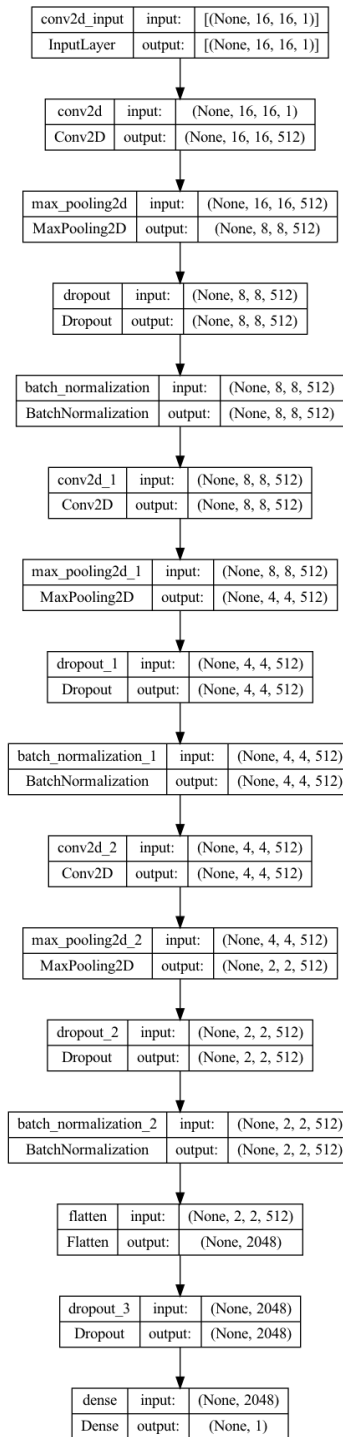


Figure 12: Model architecture for superkingdom taxonomic classifier

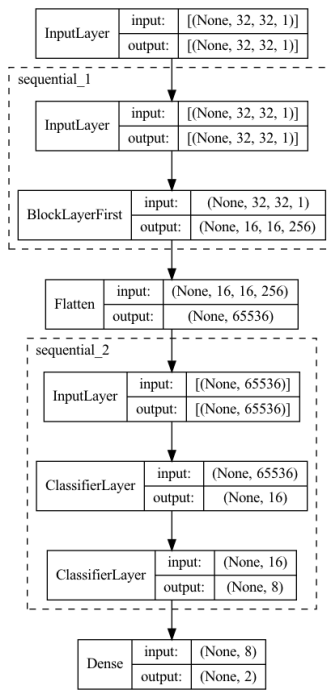


Figure 13: Model architecture for host/pathogen read classifier